

STEADY-STATE MODEL OF HETEROGENEOUS DETONATION WITH REACTIVE METALLIC PARTICLES

Alexander Gonor
Applied Science & Engineering Consulting
624-523 Finch Avenue West, Toronto, ON Canada, M2R 1N4

Irene Hooton
Defence R&D Canada Suffield
PO 4000, Stn Main, Medicine Hat, AB Canada, T1A 8K6

Shankar Narayan
Adsorption Technology Consultant
78 Stonemeadow Drive, Kanata, ON Canada K2M 2M3

A comprehensive, 1-D model of the steady-state detonation of a condensed explosive with reactive particles was developed. The model accounts for carrier, particle and oxide phases, velocities and temperatures of the carrier and particle phases, their densities, pressure, *etc.* The features of the model are: sub-models for particle vaporisation and boiling at high pressures and particle combustion, a method of determining source terms for oxygen carriers in the flow of detonation products, a sub-model for the interaction between the particle and leading shock wave front and generalisation of the conditions at the leading shock wave. The results of calculations using this model have shown that a heterogeneous mixture of RDX with ultra-dispersed aluminum particles (0.1 μm) leads to a reduction in the detonation velocity compared to its corresponding value for pure RDX or a mixture with inert particles. The ultra-dispersed particles are burned completely in the RDX reaction zone for detonations with particle mass fraction less than 20%. The model results indicate that the detonation velocity of the heterogeneous mixture decreases to a greater extent as the intensity of the heterogeneous and vapour-phase combustion of the particles is increased. An important factor affecting the decrease in detonation velocity is the reduction in mass fraction of the gaseous component of the detonation products. This parameter is reduced, on average, by ~9 to 23% when the mass fraction of the metallic particles increases from 10 to 30%. Analysis of the model results for the detonation of RDX containing 5 μ -sized aluminum particles has shown that the particles do not burn in the reaction zone.

INTRODUCTION

This paper describes the development of a comprehensive model of a steady detonation wave in a heterogeneous charge with metallic reactive particles, its various sub-models,

analysis of the numerical results for different RDX/Al mixtures and comparison with experiment. This model contains sub-models for the vaporisation of the metallic particles at high pressures, the vapour-phase and heterogeneous combustion of the particles,

and the particle interaction with the leading shock wave.

BASIC MODEL FOR THE STEADY-STATE HETEROGENEOUS DETONATION WITH REACTIVE METALLIC PARTICLES

The one-dimensional steady-state motion of a planar detonation wave in a continuous medium is considered in this model. The basic system of equations for multi-phase fluid dynamics, in the coordinate system fixed to the detonation wave, can be written in the following form,

$$\begin{aligned} \frac{d\rho_1 u_1}{dx} = J_1, \quad \frac{d\rho_2 u_2}{dx} = J_2, \quad \frac{dnu_2}{dx} = 0, \\ \rho_1 u_1 \frac{du_1}{dx} = -\frac{dp}{dx} + J_3, \quad \rho_2 u_2 \frac{du_2}{dx} = J_4, \quad (1) \\ \frac{d}{dx} [\rho_1 u_1 (e_1 + \frac{u_1^2}{2}) + \rho_2 u_2 (e_2 + \frac{u_2^2}{2}) + pu_1] = J_5, \\ \frac{d}{dx} (\rho_2 u_2 e_2) = J_6. \end{aligned}$$

Indices "1" and "2" refer to the carrier and dispersed phases, respectively. The various J_i terms denote the source terms and, the rest of the terms such as u , p , e and ρ are standard terms denoting velocity, pressure, internal energy and partial density, respectively. The multi-phase, fluid dynamic equations [Eq. (1)] along with the equations-of-state (EOS) for the condensed explosive, detonation products and particles are needed to complete the basic model equations.

In the present case, Tait's EOS is used for the undecomposed explosive and the particle interaction with the leading shock wave. The EOS suggested by Kuznetsov *et al.*¹ has been used for the detonation products. The ZND model for the reaction zone of the primary explosive was modified to take into account the effect of the particles. This modification refers to the substitution of the leading shock wave front by a generalized surface of discontinuity.

It is believed that the flow of the detonation products strips the oxide film off the particle surface, as suggested by Ref. 2. Therefore, the carrier phase can be considered to be composed of three components: 1 - the undecomposed explosive and the gaseous products (denoted by their mass-fraction, c_e), 2 - the oxide particles stripped off the surface of the metallic particles (denoted by the mass fraction, c_{ox}), and, 3 - the oxide particles formed due to the vapour-phase reaction of the metallic particles (denoted by the mass fraction, c'_{ox}). The values of c_e , c_{ox} and c'_{ox} can be determined from the following diffusion equations,

$$\frac{d[\rho_1 c^j (u_1 + w_j)]}{dx} = J_{j+6}, \quad j=1,2,3, \quad (2)$$

where $c^1 = c_e$, $c^2 = c_{ox}$ and $c^3 = c'_{ox}$. The values of w_j denote the diffusion velocities which are usually considerably lower than the corresponding convective velocity, u_1 , and will be disregarded.

The oxidizer-carriers are primarily H_2O , CO_2 and CO (and seldom O_2), and their mass fractions, denoted by c_i ($i = 1, 2$ and 3), are obtained from the following equations,

$$\frac{d[\rho_1 c_i (u_1 + w_i)]}{dx} = J_{i+9}, \quad i=1,2,3. \quad (3)$$

Thorough analysis showed that the total system of equations [Eqs. (1) - (3)] could not be closed, even if it was assumed that all the source terms (J_i) and EOS were known. It was therefore necessary to derive additional equations to close the above system of equations.

Considering a unit volume of a mixture containing undecomposed explosive, detonation products, and metal and oxide particles, the following additional equations can be derived,

$$\rho_1 = \rho^0 \alpha_1^1 / c_e, \quad \alpha_1^1 = \alpha_1 [1 - \rho_1 (1 - c_e) / (\alpha_1 \rho_c)], \quad (4)$$

where ρ^0 , ρ_c and α_1 are the true density of the detonation products (together with the undecomposed explosive), the true density of the oxide particle and the volume fraction of

the detonation products plus the undecomposed explosive and oxide particles, respectively. The term, α_1^1 , represents the volume fraction of the detonation products plus the undecomposed explosive. Therefore, Eqs. (1)-(4), along with the EOS and the source terms, form the closed system of equations.

SUB-MODEL FOR PARTICLE VAPOURISATION AND BOILING AT HIGH PRESSURES

The combustion of a particle in the reaction and expansion zones of the detonation wave of a primary explosive occurs with a high external pressure, p_g ($\sim 10^{10}$ Pa). In this case, the vapour-phase fraction at the surface of the metal particles (Al, Mg), calculated using the well-known Clausius-Clapeyron equation,

$$p_v^0 = p^* \exp(-l / RT), \quad (5)$$

was found to be negligible even at temperatures of several thousand degrees.

The derivation of the corresponding equation, taking into account the effect of external pressure, was presented in Ref 3. These results³ are necessary for the development of the particle combustion model presented below. A generalized Clausius-Clapeyron equation was obtained in the following form,

$$\frac{p_v}{p^*} \exp\left(\frac{\mu_m p_v}{RTp}\right) = \exp\left[-\left\{l - \frac{\mu_m}{\rho}(p_g - p_v^0)\right\} / (RT)\right], \quad (6)$$

where p_v^0 represents the partial vapour pressure, defined by Eq. (5), μ_m is the molecular mass of the vapour, and ρ is the density of the condensed material.

The dependence of the boiling point, T_b , on the pressure reduces to the following explicit equation,

$$T_b = \frac{l - (2\mu_m p_g / \rho)}{R \text{Log}(p^* / p_g)}, \quad (7)$$

It is interesting to note that the second term in the numerator of Eq. (7) is missing in

Clausius-Clapeyron approach. Therefore, the values of T_b predicted by Eq. (7) will be lower than the corresponding values obtained based on the Clausius-Clapeyron equation⁴.

ASYMPTOTIC SUB-MODEL FOR THE VAPOUR-PHASE AND HETEROGENEOUS COMBUSTION OF PARTICLES

The physical model for the combustion of a particle, presented below, is based on the assumption⁵ that heat and mass transfer between the particle and medium takes place inside a diffusion layer, with radius, r_1 , determined by the radius of the particle, $r_0 = d/2$, and the Nusselt number, in the form $r_1 = r_0 \text{Nu} / (\text{Nu} - 2)$.

It is assumed that both the heterogeneous and the vapour-phase reactions are first order with respect to the oxygen carriers and obey the Arrhenius temperature law,

$$\begin{aligned} k_{0i} &= k_{0i}^* \rho_1^{02} n_i^0 \exp(-E_i^0 / RT_2), \\ k_i &= k_i^* (\rho_1^0)^2 n_i n_v \exp(-E_i / RT_2), \end{aligned} \quad (8)$$

where k_{0i} and k_i are the rates with respect to the metal, k_{0i}^* and k_i^* are the reaction constants, n_i^0 and ρ_1^0 are the mass fractions of the oxygen carriers at the particle surface and density of the carrier phase in the vicinity of the particle surface, respectively, and, $\rho_1^{02} = \rho_1^0(r_0, T_2)$; n_i and n_v are the mass fractions of the oxygen carriers and metal vapour within the diffusion layer.

According to Ref. [6], a new, independent variable is introduced as,

$$z = \exp[\rho_1^{02} v_0 r_0 c_p \lambda_0^{-1} (1 - r_0 / r)] - 1, \quad r_0 \leq r \leq r_1 \quad (9)$$

where λ_0 and c_p are the thermal conductivity and specific heat, respectively.

An approximate solution to the standard system of heat transfer and diffusion equations can be found using the following series expansion: $T = T_0 + \varepsilon T_1 + \dots$, $n_i = n_{i0} + \varepsilon n_{i1} + \dots$, where $\varepsilon = n_v^0 = \mu_m / [\mu_v(1 + p_g/p_v)]$ ($\ll 1$) is a small parameter, and n_v^0 is the vapour mass fraction at the particle surface, determined

using Eq.(6), and, μ_v is the molecular mass of the surrounding gas.

A series of calculations was carried out resulting in the following correlation for n_i^0 ,

$$\begin{aligned} n_i^0 &= \frac{c_i(1-Q_i)}{1+z_1(1+D_i)}, \\ Q_i &= \frac{dn_v^0 P_{i1} \rho_1^{02} (k_i^*/k_{i0}^*) \exp[-(E_i - E_i^0)/RT_2]}{Nu z_1 (1 + \Pi_i) \text{Log}(1 + z_1)}, \\ D_i &= \frac{c_p d \rho_1^{02} \beta_i k_{i0}^* \exp(-E_i^0 / RT_2)}{\lambda_0 Nu \text{Log}(1 + z_1)}. \end{aligned} \quad (10)$$

where, $Q_i \leq 1$, $\Pi_i D_i = (1+z_1)/z_1$, $z_1 = z(r_1)$ and β_i is the stoichiometric ratio. The term $P_{i1} = P_i(z_1)$, where $P_i(z)$ is a given polynomial. For values of Q_i in Eq. (10) greater than 1, the equality $Q_i = 1$ is used. Finally, the function $z_1(x)$ is found using the following equation,

$$\sum_{i=1}^N \left[\frac{Q_i}{\beta_i} - \frac{1-Q_i}{1+\Pi_i} \right] c_i + n_v^0 (1+z_1) - z_1 = 0, \quad (11)$$

The parameters, E_i^0 and E_i , in Eq. (10), are activation energies for heterogeneous and vapour-phase reactions, respectively. In the calculations below, it is assumed $E_i^0 = E_i$. It is important to note that the value of the ratio k_i^*/k_{i0}^* , the ratio of the rate constants of the vapour-phase reaction to the corresponding value for the heterogeneous reaction of the metallic particle, in Eq. (10) are unknown. In order to overcome this limitation, it is assumed that only the vapour-phase combustion of the particle occurs at its boiling point, therefore, $Q_i=1$ since $n_i^0=0$. This assumption facilitates the exclusion of the ratio k_i^*/k_{i0}^* from Eq. (10).

Therefore, the sub-model for particle combustion reduces to Eq. (11) with respect to the function $z_1(x)$, which is solved simultaneously with the general system of equations (1) – (3).

SUB-MODEL FOR PARTICLE INTERACTION WITH THE LEADING SHOCK FRONT OF A DETONATION

To estimate the particle and flow

parameters behind the leading shock wave, a 1-D method of the break-up of the arbitrary discontinuity and (mass, momentum and energy) balance equations at the shock wave was used. Overall, nine equations were obtained for nine unknown parameters, namely, u_i , ρ_i , T_i , ($i = 1,2$), p , n and α_1 , which allowed the calculation of their dependencies on the detonation velocity, D , and particle mass fraction, m_2 . Calculations of all carrier phase and particle parameters behind the leading shock wave were carried out, in the system of coordinates attached to the shock wave, with the following parameters, $4000 \leq D \leq 10000$ m/s, $0 \leq m_2 \leq 0.4$.

It appears the detonation velocity is very sensitive to values of the output parameters that are the boundary conditions for the system of equations (1). As a result, the numerical 2-D modeling of the shock wave diffraction over a spherical compressible particle (Al and Mg) in RDX, with the HOM EOS was produced⁷. The results were compared with data from the 1-D approach. The values for particle temperature, T_2^1 , are shown in Fig. 1 by the solid circles, corresponding to the 2-D numerical method for RDX ($\rho = 1.4$ g/cm³) with Al particles. The solid line, obtained from 1-D approach, displays good agreement with the numerical modeling.

A comparison of the ratio of the absolute particle velocity with the flow velocity, obtained with the 2-D numerical method and using modified the 1-D approach, yields comparable results as well.

VARIOUS SOURCE TERMS AND CORRELATIONS REQUIRED TO OBTAIN A CLOSED SOLUTION

The mass fluxes between the carrier and dispersed phases, denoted by J_1 and J_2 , respectively, are related by the condition $J_1 = -J_2$. The mass flux consists of three components, 1) the flux of the oxides formed

due to the heterogeneous combustion of the metal particles, denoted by J_c , 2) the flux of the metal vapour formed due to its evaporation, denoted by J_m , and, 3) the flux of oxygen into the dispersed phase, denoted by J_0 . In the case of a stoichiometric reaction between the metallic particle and the oxidizer, the flux J_0 can be written as, $J_0 = \nu_0 J_c$, where ν_0 denotes the stoichiometric ratio. Therefore, J_1 can be written as the following correlation,

$$J_1 = J_m + (1 - \nu_0) J_c, \text{ for } T_0 \leq T_2 \leq T_b \quad (12)$$

The mass flux of the metal vapour due to evaporation from the surface of the particle, J_m , can be determined by the following equation,

$$J_m = 6\alpha_2 [\lambda_0 Nu \text{Log}(1 + z_1)] / (c_p d) + \rho_1^{02} \sum_{i=1}^N \beta_i k_{0i}^* n_i^0 \exp(-E_i^0 / RT_2) / d \quad (13)$$

The Nusselt number is given by a well-known expression⁸, as a function of Mach, Reynolds and Prandtl numbers. Assuming the rates of the heterogeneous reactions are represented by the formulae given in Eq. (8), the source term J_c can be represented by the following equation,

$$J_c = 6\alpha_2 \nu_c \rho_1^{02} \left[\sum_{i=1}^N k_{0i}^* n_i^0 \exp(-E_i^0 / RT_2) \right] / d, \quad (14)$$

where ν_c denotes the stoichiometric ratio for the heterogeneous combustion of Al to Al_2O_3 .

The next step is to determine the forces of interaction between the interfaces, defined by the momentum flux terms, J_3 and J_4 . The drag coefficient is determined by the following correlation, proposed by Henderson, $C_D = (24/\text{Re})L_D$. A detailed description of the function $L_D(M, \text{Re})$ can be found in Ref. [9].

It is important to note that the total resistance to flow by the particles comprises of not only the drag force, but also the forces of the apparent masses and the Archimedes force. Taking into account all these forces, the source terms for the momentum flux, J_3 and J_4 , can be represented by the following,

$$J_3 = -\frac{\alpha_2 \rho_1}{2\alpha} \left[\frac{3}{2d} C_D (u_1 - u_2) |u_1 - u_2| - u_2 \frac{du_2}{dx} + 3u_1 \frac{du_1}{dx} \right] - (u_1 - u_2) J_1, \\ J_4 = -J_3 - (u_1 - u_2) J_1. \quad (15)$$

The specific internal energy of the carrier phase, with oxide particles, e_1 , can be represented by the following equation,

$$e_1 = c_e (e + ZQ) + (1 - c_e) e_c - c_{ox}' q_c, \quad (16)$$

where e , e_c , Z , Q and q_c denote the specific internal energy of the detonation products plus undecomposed explosive, the specific energy of the oxides, the mass fraction of the undecomposed explosive, the heat of reaction of the primary HE and the heat of the vapour-phase particle reaction, respectively.

The specific internal energy of the particles considered incompressible, denoted by e_2 , can be determined from the following co-relations,

$$e_2 = \alpha_m T_2, T_0 \leq T_2 \leq T_m \text{ or } \alpha_m T_m + wL, T_2 = T_m \text{ or } \alpha_m T_2 + L, T_m \leq T_2 \leq T_b.$$

Here T_m and L denote the melting point and latent heat of melting of the particles, and w [=m/m_p] denotes the fraction of the particle which has melted.

The energy source term, J_5 , including the radiation effect caused by particles, is given by the following,

$$J_5 = 6\alpha_2 \varepsilon \sigma (T_1^4 - T_2^4) / d + J_c q_c, \quad (17)$$

The next step is to determine the last source term, J_6 , in the system of equations, given by Eqs. (1). J_6 is given by the following equation,

$$J_6 = 6\alpha_2 \{ \lambda_0 Nu \text{Log}(1 + z_1) [T_1 - T_2 - (q/c_p)(n_v^0(1 + z_1) - z_1)] / z_1 + q d \rho_1^{02} \sum_{i=1}^N \beta_i k_{0i}^* n_i^0 \exp(-E_i^0 / RT_2) + \varepsilon \sigma d (T_1^4 - T_2^4) \} / d^2 \\ + J_c (q_c - e_c|_{T_2} + \nu_0 e_0) - J_m (e_2 + l). \quad (18)$$

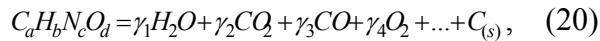
Besides the source terms, J_1 - J_6 , the system of model equations, given by Eqs. (2) and (3), also contains six other unknown source terms. It can be stated that $J_8 = J_c$ and $J_9 = \nu_c J_m$. The source term, J_9 , is developed based on the assumption that the total conversion of all the metal vapour into the oxide is accomplished. Therefore, from Eq. (2), the source term, $J_7 = (1 - \nu_c) J_1$.

The rate of decomposition of the primary HE is assumed to be represented by the Arrhenius rate law in terms of the following correlation,

$$u_1 d(c_e Z) / dx = -c_e Z [a \exp(-E / RT_1) + J_1 / \rho_1], \quad (19)$$

For a pure explosive, $c_e=1$ and $J_1=0$; and Eq. (19) reduces to the well-known form of the Arrhenius rate law.

The remaining source terms, J_{10} - J_{12} , have been determined based on the following hypothesis. For a primary explosive, represented by $C_a H_b N_c O_d$, the overall detonation reaction at the C-J point can be represented by the following chemical reaction¹⁰,



that leads to the following equality, $\sum_{i=1}^{N_i} \gamma_i \mu_i / \mu_e = 1$,

where μ_e and μ_i denote the molecular masses of the primary explosive and the detonation products (such as H_2O , CO_2 , CO etc.), and γ_i denotes the number of moles of the corresponding product component, as given in Eq. (20). Every term on the left side of this equality represents the mass fraction of the corresponding species of the detonation products. It is assumed that these values for the mass fraction can be used at various intermediate points in the reaction zone. As a result, the source terms for various oxygen carriers can be represented by the following equation,

$$J_{i+9} = c_e \rho_1 Z (\gamma_i \mu_i / \mu_e) a \exp(-E / RT_1) + 6\alpha_2 \lambda_0 Nu \log(1+z_1) \times [c_i - (1+z_1)(dn_i/dx)_{z_1}] / (c_p d^2), \quad i=1,2,3 \quad (21)$$

The first term in Eq. (21) represents the flux of the oxygen carrier, produced by the decomposition reaction of the primary explosive, and the second term represents its consumption due to the heterogeneous and vapour-phase reactions between the oxygen carrier and the metal particle.

The "shooting" method, using the solutions for different values of the detonation velocity, was implemented to obtain the true solution.

MODEL RESULTS AND THEIR ANALYSIS FOR HETEROGENEOUS DETONATIONS WITH RDX CONTAINING ULTRADISPERSED

ALUMINUM PARTICLES

As a first effort, a series of runs was conducted to predict profiles of various parameters for detonations with medium-density (1.4 g/cm^3) RDX containing $0.1\text{-}\mu\text{m}$ diameter Al particles in mass fractions (m_2) ranging from 0.1 to 0.3. The ranges of the values for various rate constants, k_{oi}^* , were selected as following:

$$H_2O: k_{01}^* = 14 \cdot 10^3 \div 140 \text{ m/s}, \quad CO_2: k_{02}^* = 4.1 \cdot 10^3 \div 41 \text{ m/s}, \\ CO: k_{03}^* = 5 \cdot 10^2 \div 5 \text{ m/s}.$$

An initial set of runs with $m_2=0.1$ indicated that for the maximum values of the rate constants, k_{oi}^* , shown above, a steady-state detonation did not exist. To obtain a steady-state solution, the values of k_{oi}^* were reduced to one-tenth and one hundredth of their maximum value. The results from the reduced values of the parameters exhibited a steady detonation wave with a VOD of 6928 m/s for the minimum values of the rate constants. It is interesting to note that a decrease in the VOD of ~ 500 m/s, as the particle mass fraction increased from 0 to 10%, corresponds, qualitatively, relatively well with some of the experimental data reported in Refs. [11 and 12]. Note the VOD continuously decreases from 7429 m/s to 6203 m/s as the particle mass concentration is increased from 0 to 30%.

Profiles of the temperatures of the carrier and dispersed phases, T_1 and T_2 respectively, are given in Figs. 2 and 3. The flow temperature, T_1 , increases sharply close to the leading shock wave and then decreases, particularly in cases of mixtures with higher Al concentrations (e.g. $m_2=0.2$ and 0.3). Subsequently, T_1 increases to its maximum value at the point where the decomposition of the primary explosive is complete. It should be noted that the flow temperatures in the front part of the reaction zone for detonations of Al mixtures are significantly lower than the corresponding value for pure RDX, and the difference increases with increasing mass

concentration of the particles. However, the values of T_1 throughout the reaction zone are significantly greater for detonations with mixtures than corresponding values for pure RDX, which contributes additional explosive energy. The distribution of the particle temperature, T_2 , as shown in Fig. 3, indicates that the particles are heated very rapidly. The temperature of the particles does not reach the boiling point and begins to decrease after reaching a maximum, as the particle size is reduced to zero.

The addition of the particles also results in a significant change in the pressure profile within the reaction zone. Instead of a gradual decrease in pressure, as observed for pure RDX (Fig. 4), it can be observed that there is a sharp increase in pressure close to the leading shock wave front, followed by a region of fairly gradual decrease, to a point where there is a sharp decrease in the pressure, followed by another region of fairly gradual decrease in the expansion zone. Overall, the maximum values of pressure and partial density are less for RDX/Al mixtures than those for pure RDX.

The profiles of c_e within the reaction zone, as shown in Fig. 5, indicate a significant reduction in the gaseous component of the detonation products. For example, the average c_e in the reaction zone is predicted to decrease by ~9%, 19% and 23% as the mass concentration of particles in the HE is increased to 10%, 20% and 30%, respectively. It is believed that a significant reduction in the concentration of ($c_e \rho_1$), along with the energy and momentum losses due to the particles, are the primary factors causing the decrease in detonation velocity due to the addition of the reactive metallic particles. It is interesting to note that the experimental results in Ref. [11], allowed its author to conclude that the decrease in VOD from the detonation of pure explosive, compared to one involving mixtures with reactive particles, was greater than the corresponding decrease in detonations

involving mixtures with inert particles. This behaviour is understandable if the reduction in the gaseous concentration of the carrier phase in the case of reactive particles is considered, whereas, a similar reduction does not occur in the case of inert particles.

The distribution of the mass fraction of oxide particles, c'_{ox} , produced by vapour-phase combustion is shown in Fig. 6. For $m_2=0.1, 0.2$ and 0.3 , the mass fractions of particles burned in the vapour-phase reaction, were calculated to be ~6.3%, 4.4% and 3.8%, respectively. This indicates that the vapour-phase combustion of the particle at high pressures within the reaction zone is not very effective.

It should be noted that the important part of the heterogeneous detonation process is the mass fraction of oxygen-carriers in the detonation products, c_i , namely, H_2O , CO_2 and CO . The distribution of c_1 (H_2O) is shown in Fig. 7. In accordance with the total decomposition of the primary explosive (RDX), the values of mass fraction, c_1 , as expected, reach a maximum, and then, particularly when $m_2 > 0.15$, the mass fraction of the oxygen-carrier starts decreasing, signifying the consumption of this carrier due to the fact that the combustion of the particles exceeds its production by the decomposition of RDX.

The distribution of the mass fraction of the oxygen carrier, H_2O , at the surface of the particle, denoted by n_1^0 , is shown in Fig. 8. This distribution clearly indicates the combustion reaction at the particle surface occurs with mass fractions of the oxygen-carrier (H_2O) significantly lower than corresponding values in the detonation products.

The variation in particle size in terms of its diameter, d_p , within the reaction zone is shown in Fig. 9. It is important to note that for $m_2 < 0.2$, the particles are burned completely within the reaction zone. In the case of $m_2 = 0.25$, the combustion of the particles is not

completed within the reaction zone.

MODEL RESULTS FOR THE HETEROGENEOUS DETONATION OF RDX/AL MIXTURES CONTAINING MICRON-SIZED REACTIVE PARTICLES

The profiles of various parameters within the reaction zone were calculated for the detonation of moderate density (1.4 and 1.56 g/cm³) RDX explosives containing 5- μ m diameter aluminum particles. The results from the model for the detonation of a RDX/Al mixture containing a 10% mass fraction of Al particles ($m_2=0.1$), in terms of the distribution of all flow and particle parameters were obtained.

The distribution of the particle velocity, u_2 , and flow velocity, u_1 , shows that u_2 in the reaction zone is greater than u_1 , and the difference between them reduces to almost zero (~ 38 m/s) near the C-J plane. The pressure distribution for this example, as shown in Fig. 10, is similar to that obtained for pure RDX. However, over a large area of the reaction zone, the pressure, for detonations with reactive particles, is lower than the corresponding value for detonations of pure explosive due to losses to the particles.

The flow temperature with reactive particles is 600-800 K higher than that for pure RDX. This increase in temperature can be attributed to two factors namely, a slightly higher value for VOD and the retardation of the particles, resulting in the heating of the flow phase. It is to be noted that the particle temperature reaches its melting point but the melting process is not complete within the reaction zone.

For detonations with mixtures having 5- μ m diameter Al particles, the particle diameter remains the same throughout the entire reaction zone. From results calculated with this model, it can be concluded that the 5- μ m diameter particles behave as inert particles in

the reaction zone. The small increase in VOD observed for detonations of RDX containing 5- μ m diameter reactive Al particles, compared to the corresponding value for pure RDX, as predicted by this model, can be explained with the same reasoning used to describe similar results for inert particles¹³. It is important to note that according to Ref. [13], depending on the HE and the equation-of-state (EOS), the exact opposite behaviour, *i.e.* a decrease in VOD with the addition of 5- μ m diameter particles, could also be obtained.

CONCLUSIONS

To summarize, it can be concluded that the steady-state heterogeneous detonation model results are viable; and it has been convincingly demonstrated that the increase in VOD for explosive mixtures involving the combustion of metallic particles is negligible, or almost impossible, and, in the majority of cases, a decrease in VOD occurred. Two factors in this model have the greatest impact on the values of VOD and the structure of the reaction zone. The first factor is the values of the initial flow parameters (temperature, density, *etc.*) behind the leading shock wave, which depends on particle mass fraction and EOS of the condensed HE. The second is the values of rate constants for heterogeneous and vapour-phase reactions of Al particles with the oxygen carriers.

The primary effect of the heterogeneous explosion is amplification of the blast wave, as a result of a higher flow temperature compared with the explosion of pure HE. Analysis of the results from a series of experimental tests has shown a definite decrease in VOD for mixtures containing RDX with ultradispersed particles and a slight decrease in the VOD for mixtures containing (5 μ m) micron-sized particles. These results are in agreement with the predictions obtained from this model.

ACKNOWLEDGEMENTS

This work was supported under the auspices of the DND contract W7708-8-R748

REFERENCES

1. Kuznetsov, V. M., Kuznetsov N. M. and Shatsukevich A. F., *Equation of State and Isentropy of the Detonation Products of Typical Condensed Explosives*, Combustion, Explosion and Shock Waves, v. 18, No. 1, 1982, pp. 98-101.
2. Davydov, V. Yu. et al., *Experimental-Theoretical Study of Aluminum Oxidation in Detonation Wave*, Combustion, Explosion and Shock Waves, v. 28, No. 5, 1992, p.124.
3. Gonor, A. L., *High Pressure Vaporization and Boiling of Condensed Material: A Generalized Clausius-Clapeyron Equation*, in Shock Compression of Condensed Matter - 2001, edited by M. Furnish (Elsevier, New York, to be published), Conference Proceedings.
4. Glassman, I., *Combustion of Metals: Physical Considerations*, Progress in Astronautics and Rocketry Series, edited by M. Summerfield, v. 1, Academic Press: New York, 1960, p.253.
5. Frank-Kamenetskii, D. A., *Diffusion and Heat Transfer in Chemical Kinetics*, Plenum Press: New York - London, 1969, pp.29-35.
6. Gurevich, M. A. and Stepanov, A. M., *Ignition Limits of a Metal Particle*, Combustion, Explosion and Shock Waves, v. 4, No. 2, 1968, pp.109-112.
7. Zhang, F., Thibault, P.A., Link, R., and Gonor, A.L., *Momentum Transfer during Shock over Metal Particles in Condensed Explosives*, in Shock Compression of Condensed Matter - 2001, edited by M. Furnish (Elsevier, New York, to be published), Conference Proceedings.
8. Fox, T. W. et al., 11th International Symposium on Shock Tubes and Waves, University of Washington Press: Seattle, 1977, pp. 262-268.
9. Henderson, C. B., *Drag Coefficients of Spheres in Continuum and Rarefied Flow*, AIAA Journal, v. 14, No. 6, 1976, pp. 707-708.
10. Mader, C. L., *Numerical Modeling of Explosives and Propellants*, 2nd Edition. CRC Press: New York, 1998, pp.53-54
11. Aniskin, A. I., *Detonation of Explosive Mixtures with Aluminum*, Proceedings of VIII All Union Symposium on Combustion and Explosion: Chernogolovka (USSR) 1989, pp.26-32.
12. Baudin, G., *Combustion of Nanophase Aluminum in the Detonation Products of Nitromethane*, 11th International Symposium on Detonation, ONR: Snowmass Village, Colorado, 1998, pp.1-9.
13. Gonor, A. L., Hooton, I., Narayan, S. B., *Steady-State Model of Heterogeneous Detonation with Inert Particles*, in Shock Compression of Condensed Matter - 2001, edited by M. Furnish (Elsevier, New York, to be published), Conference Proceedings.

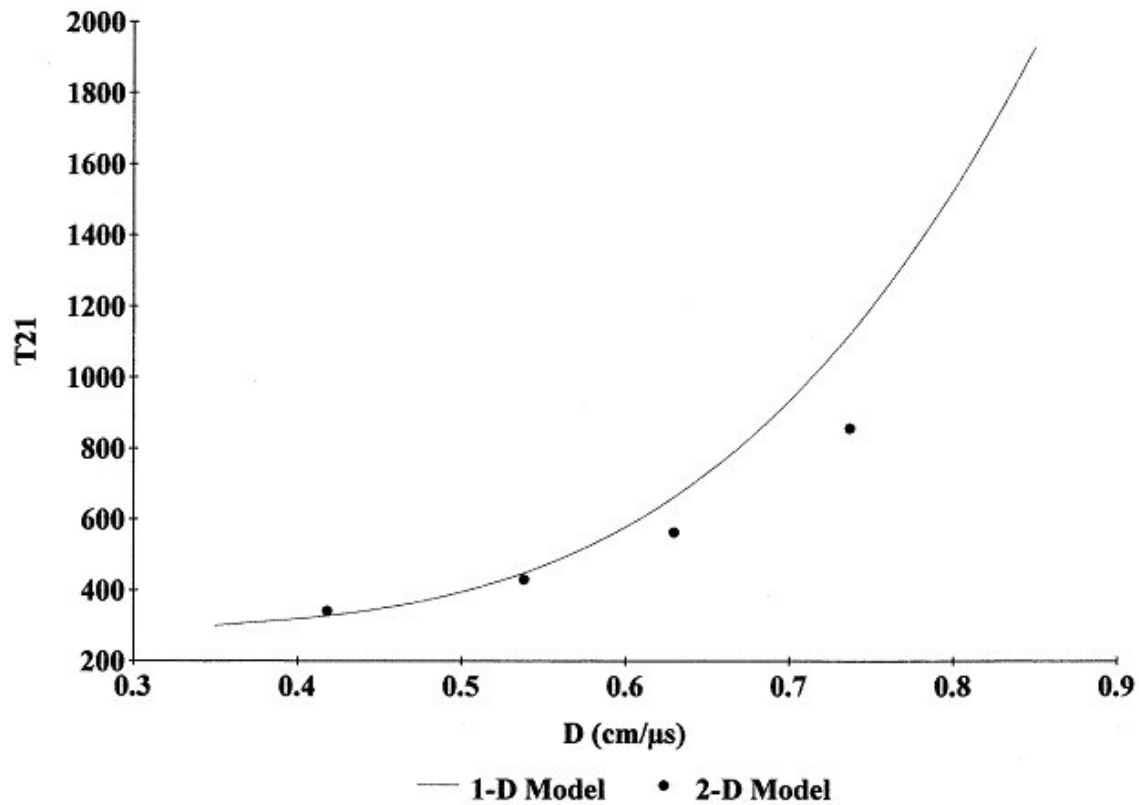


FIGURE 1. T_2^1 AS A FUNCTION OF D

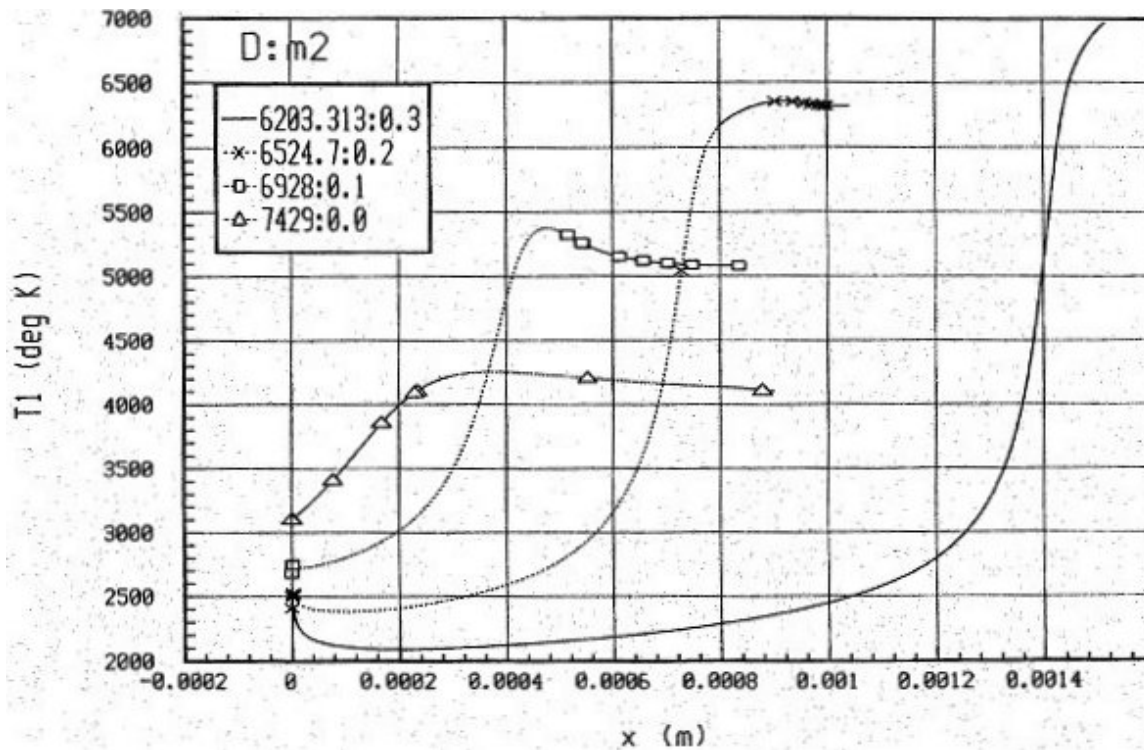


FIGURE 2. T_1 -DISTRIBUTION FOR RDX/AL MIXTURES (1.4 g/cm³, 0.1 μ m)

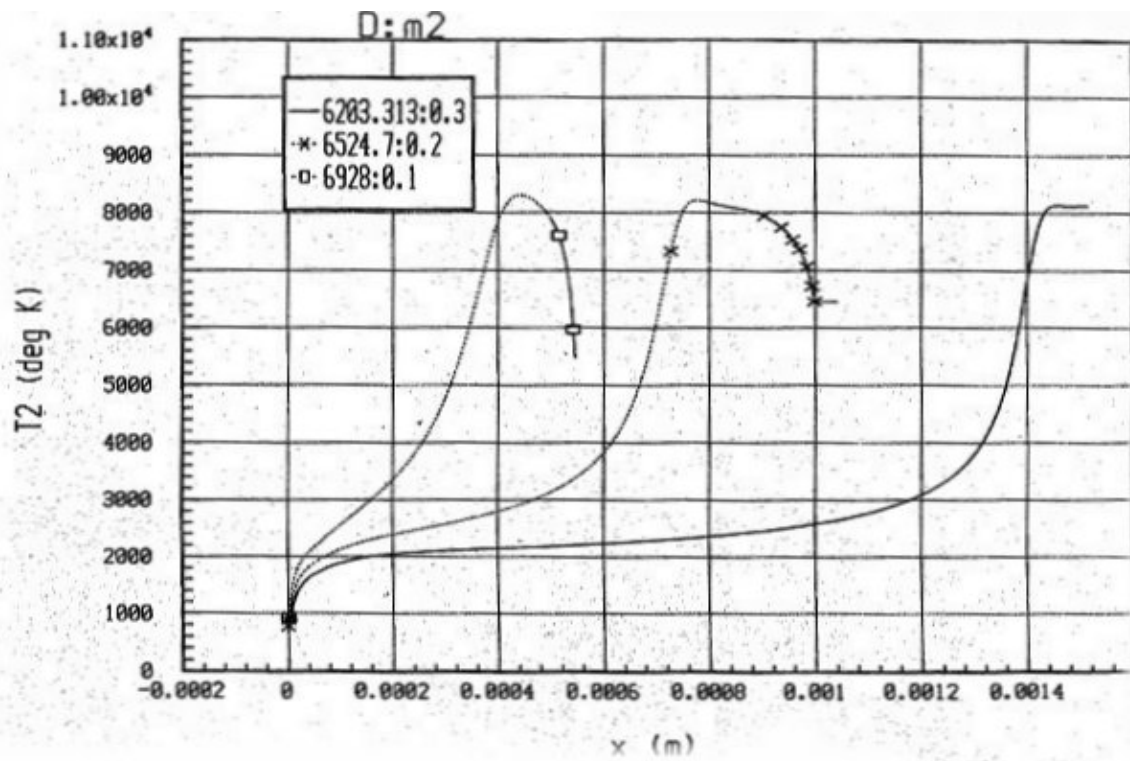


FIGURE 3. T₂-DISTRIBUTION FOR RDX/AL MIXTURES (1.4 g/cm³, 0.1 μm)

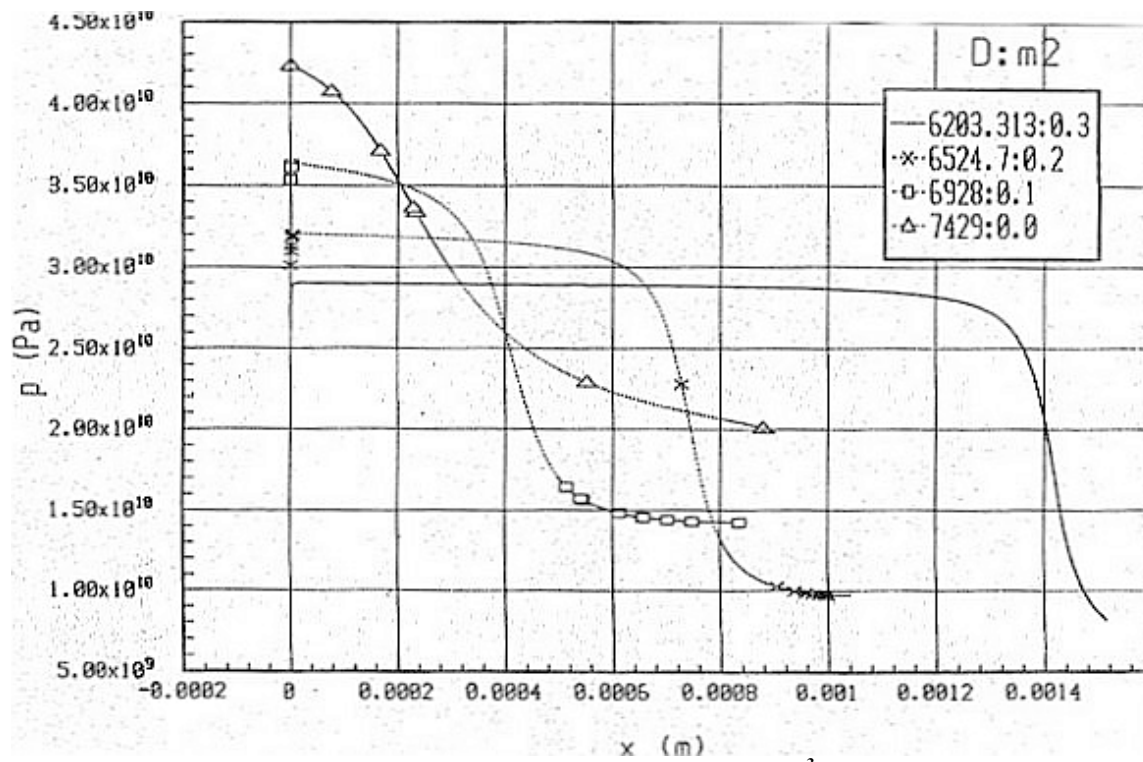


FIGURE 4. P-DISTRIBUTION FOR RDX/AL MIXTURES (1.4 g/cm³, 0.1 μm)

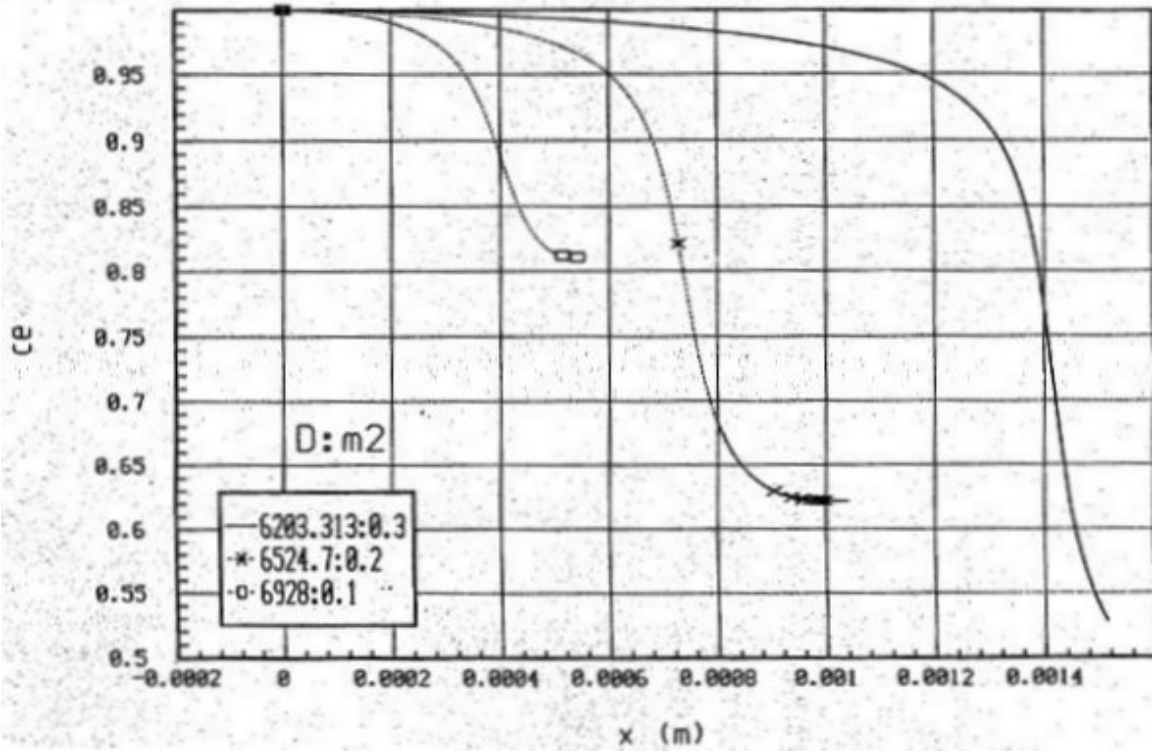


FIGURE 5. C_e -DISTRIBUTION FOR RDX/AL MIXTURES (1.4 g/cm^3 , $0.1 \mu\text{m}$)

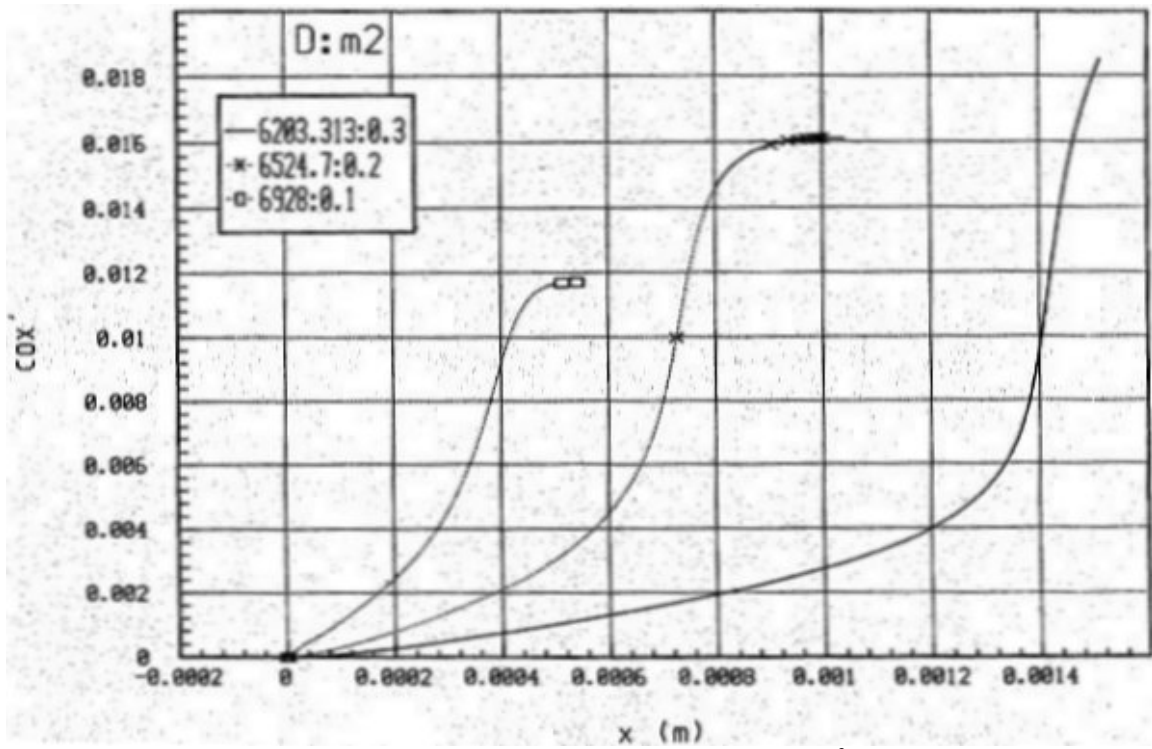


FIGURE 6. C'_{ox} -DISTRIBUTION FOR RDX/AL MIXTURES (1.4 g/cm^3 , $0.1 \mu\text{m}$)

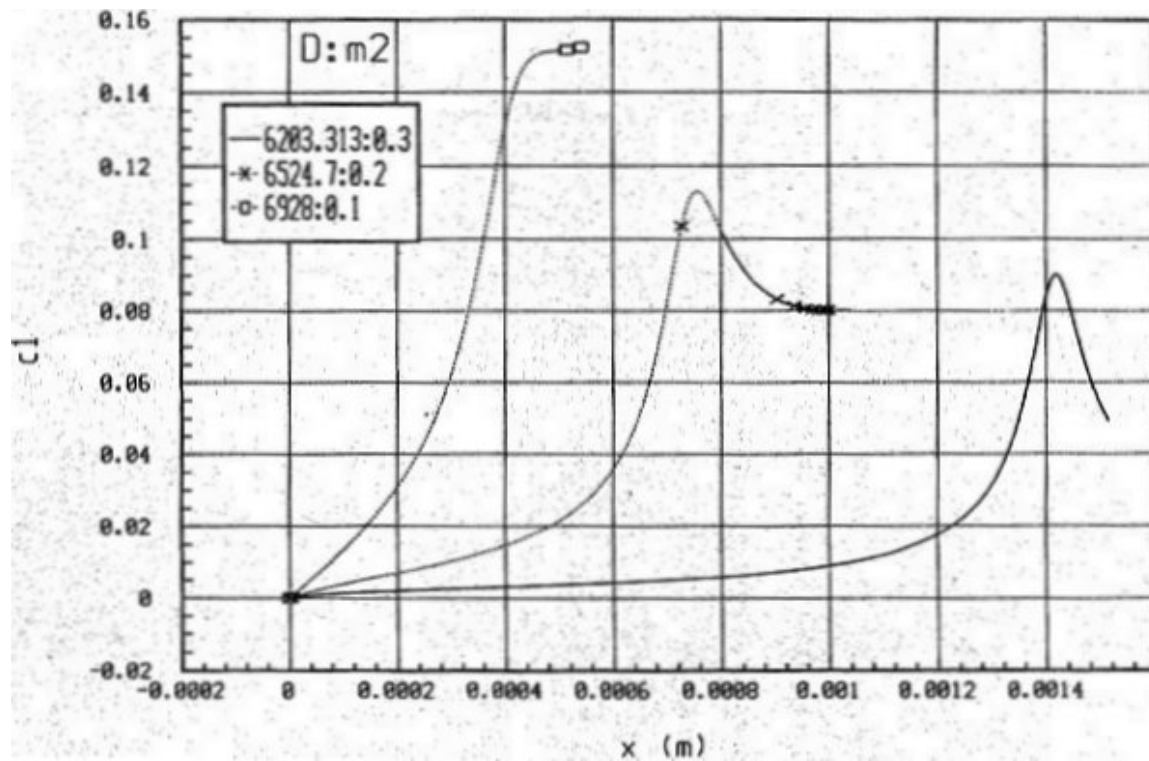


FIGURE 7. C_1 -DISTRIBUTION FOR RDX/AL MIXTURES (1.4 g/cm^3 , $0.1 \mu\text{m}$)

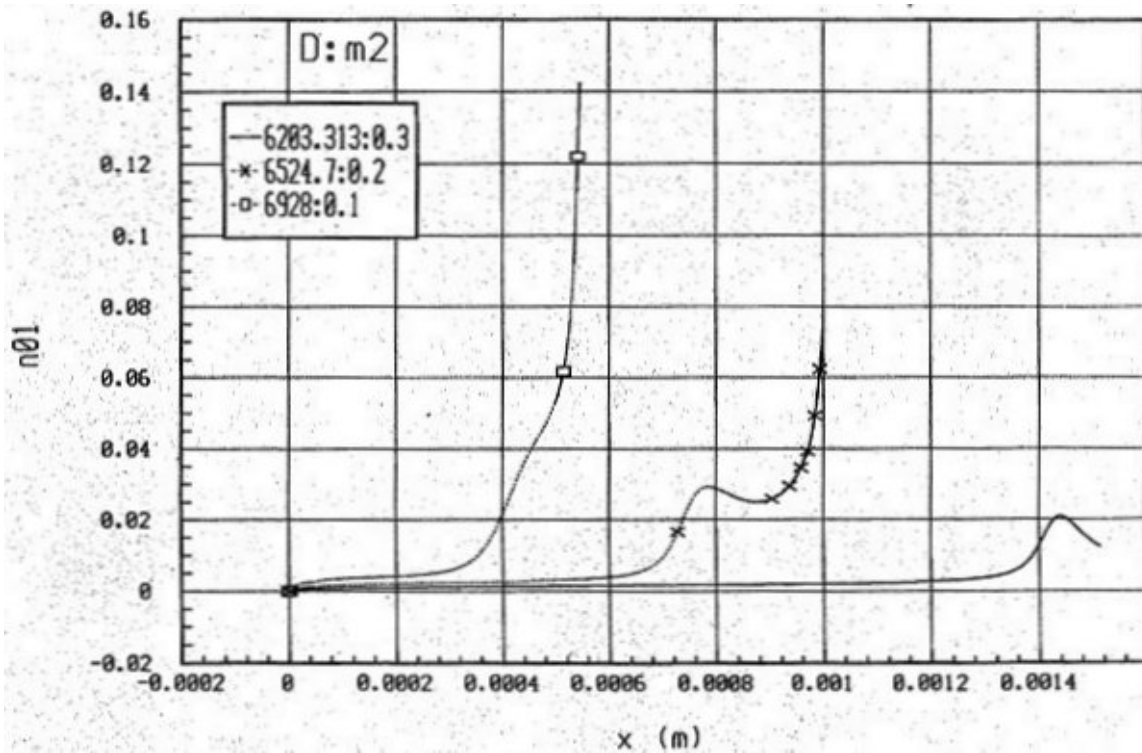


FIGURE 8. n_1^0 -DISTRIBUTION FOR RDX/AL MIXTURES (1.4 g/cm^3 , $0.1 \mu\text{m}$)

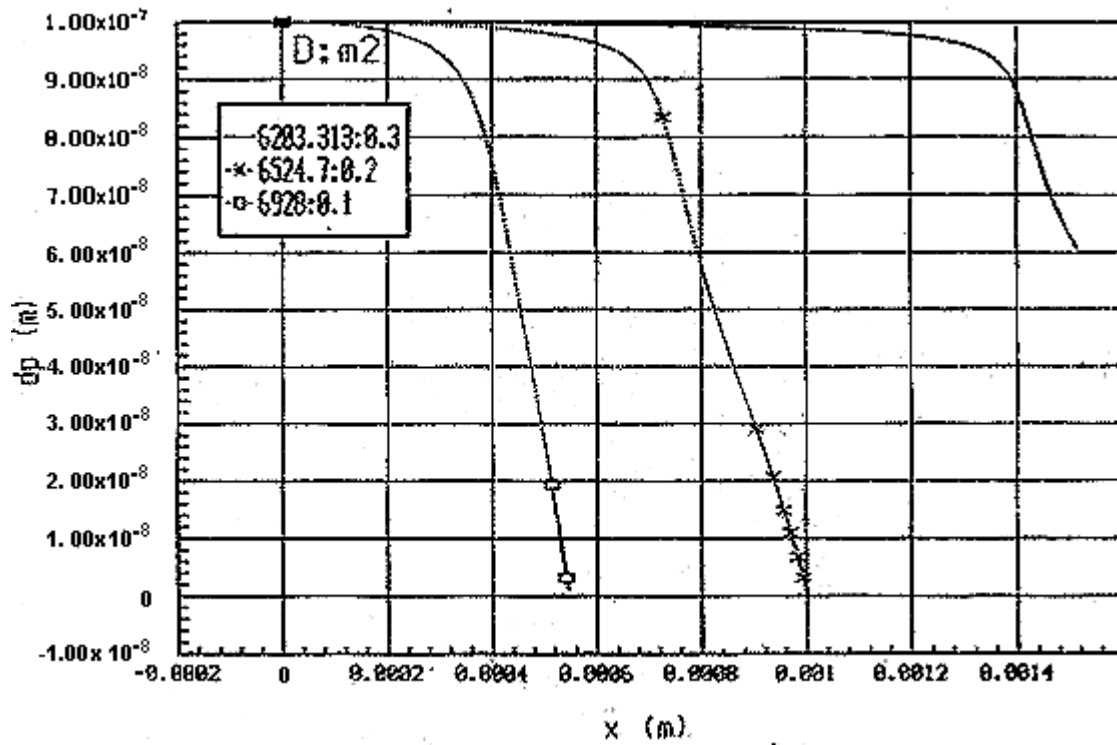


FIGURE 9. d_p - DISTRIBUTION FOR RDX/AL MIXTURES (1.4 g/cm^3 , $0.1 \mu\text{m}$)

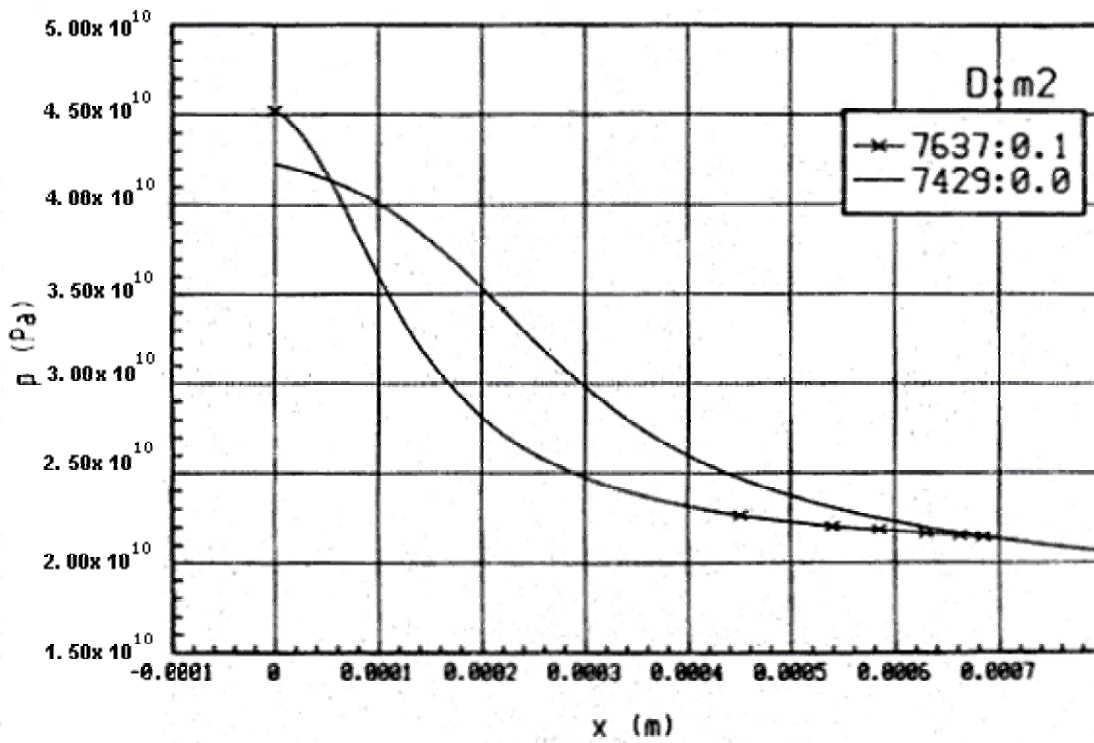


FIGURE 10. P - DISTRIBUTION FOR RDX/AL MIXTURES (1.4 g/cm^3 , $5.0 \mu\text{m}$)

EQUATIONS

$$\begin{aligned} \frac{d\rho_1 u_1}{dx} &= J_1, \quad \frac{d\rho_2 u_2}{dx} = J_2, \quad \frac{dnu_2}{dx} = 0, \\ \rho_1 u_1 \frac{du_1}{dx} &= -\frac{dp}{dx} + J_3, \quad \rho_2 u_2 \frac{du_2}{dx} = J_4, \\ \frac{d}{dx} [\rho_1 u_1 (e_1 + \frac{u_1^2}{2}) + \rho_2 u_2 (e_2 + \frac{u_2^2}{2}) + pu_1] &= J_5, \\ \frac{d}{dx} (\rho_2 u_2 e_2) &= J_6. \end{aligned} \quad (1)$$

$$\frac{d[\rho_1 c^j (u_1 + w_i)]}{dx} = J_{j+6}, \quad j=1,2,3, \quad (2)$$

$$\frac{d[\rho_1 c_i (u_1 + w_i)]}{dx} = J_{i+9}, \quad i = 1,2,3. \quad (3)$$

$$\rho_1 = \rho^0 \alpha_1^1 / c_e, \quad \alpha_1^1 = \alpha_1 [1 - \rho_1 (1 - c_e) / (\alpha_1 \rho_c)], \quad (4)$$

$$p_v^0 = p^* \exp(-l / RT), \quad (5)$$

$$\frac{P_v}{p^*} \exp\left(\frac{\mu_m P_v}{RTp}\right) = \exp\left[-\left\{l - \frac{\mu_m}{\rho} (p_g - p_v^0)\right\} / (RT)\right], \quad (6)$$

$$T_b = \frac{l - (2\mu_m P_g / \rho)}{R \text{Log}(p^* / p_g)}, \quad (7)$$

$$\begin{aligned} k_{0i} &= k_{0i}^* \rho_1^{02} n_i^0 \exp(-E_i^0 / RT_2), \\ k_i &= k_i^* (\rho_1^0)^2 n_i n_v \exp(-E_i / RT_2), \end{aligned} \quad (8)$$

$$z = \exp[\rho_1^{02} v_0 r_0 c_p \lambda_0^{-1} (1 - r_0 / r)] - 1, \quad r_0 \leq r \leq r_1 \quad (9)$$

$$\begin{aligned} n_i^0 &= \frac{c_i (1 - Q_i)}{1 + z_1 (1 + D_i)}, \\ Q_i &= \frac{dn_v^0 P_{i1} \rho_1^{02} (k_i^* / k_{0i}^*) \exp[-(E_i - E_i^0) / RT_2]}{Nu_{\bar{z}} (1 + \Pi_i) \text{Log}(1 + z_1)}, \end{aligned} \quad (10)$$

$$D_i = \frac{c_p d \rho_1^{02} \beta_i k_{0i}^* \exp(-E_i^0 / RT_2)}{\lambda_0 Nu \text{Log}(1 + z_1)}.$$

$$\sum_{i=1}^N \left[\frac{Q_i}{\beta_i} - \frac{1 - Q_i}{1 + \Pi_i} \right] c_i + n_v^0 (1 + z_1) - z_1 = 0, \quad (11)$$

$$J_1 = J_m + (1 - \nu_0)J_c, \text{ for } T_0 \leq T_2 \leq T_b \quad (12)$$

$$J_m = 6\alpha_2[\lambda_0 Nu \text{Log}(1 + z_1)] / (c_p d) + \rho_1^{02} \sum_{i=1}^N \beta_i k_{0i}^* n_i^0 \exp(-E_i^0 / RT_2) / d \quad (13)$$

$$J_c = 6\alpha_2 \nu_c \rho_1^{02} [\sum_{i=1}^N k_{0i}^* n_i^0 \exp(-E_i^0 / RT_2)] / d, \quad (14)$$

$$J_3 = \frac{\alpha_2 \rho_1}{2\alpha_1} \frac{3}{2d} C_D (u_1 - u_2) |u_1 - u_2| - u_2 \frac{du}{dx} + 3u_1 \frac{du}{dx} - (u_1 - u_2) J_1, \\ J_4 = -J_3 - (u_1 - u_2) J_1. \quad (15)$$

$$e_1 = c_e (e + ZQ) + (1 - c_e) e_c - c'_{ox} q_c, \quad (16)$$

$$e_2 = \alpha_m T_2, T_0 \leq T_2 \leq T_m \text{ or } \alpha_m T_m + wL, T_2 = T_m \text{ or } \alpha_m T_2 + L, T_m \leq T_2 \leq T_b.$$

$$J_5 = 6\alpha_2 \varepsilon \sigma (T_1^4 - T_2^4) / d + J_c q_c, \quad (17)$$

$$J_6 = 6\alpha_2 \{\lambda_0 Nu \text{Log}(1 + z_1) [T_1 - T_2 - (q / c_p) (n_v^0 (1 + z_1) - z_1)] / z_1 + q d \rho_1^{02} \sum_{i=1}^N \beta_i k_{0i}^* n_i^0 \exp(-E_i^0 / RT_2) + \varepsilon \sigma d (T_1^4 - T_2^4)\} / d^2 + \quad (18) \\ J_c (q_c - e_c |_{T_2} + \nu_0 e_0) - J_m (e_2 + l)$$

$$u_1 d (c_e Z) / dx = -c_e Z [a \exp(-E / RT_1) + J_1 / \rho_1], \quad (19)$$

$$C_a H_b N_c O_d = \gamma_1 H_2 O + \gamma_2 CO_2 + \gamma_3 CO + \gamma_4 O_2 + \dots + C_{(s)}, \quad (20)$$

$$\sum_{i=1}^{N_1} \gamma_i \mu_i / \mu_e = 1,$$

$$J_{i+9} = c_e \rho_1 Z (\gamma_i \mu_i / \mu_e) a \exp(-E / RT_1) + 6\alpha_2 \lambda_0 Nu \text{Log}(1 + z_1) \times [c_i - (1 + z_1) (dn_i / dx)_{z_1}] / (c_p d^2), i = 1, 2, 3, \quad (21)$$

$$H_2O: k_{01}^* = 14 * 10^3 \div 140 m/s, CO_2: k_{02}^* = 4.1 * 10^3 \div 41 m/s, \\ CO: k_{03}^* = 5 * 10^2 \div 5 m/s.$$

